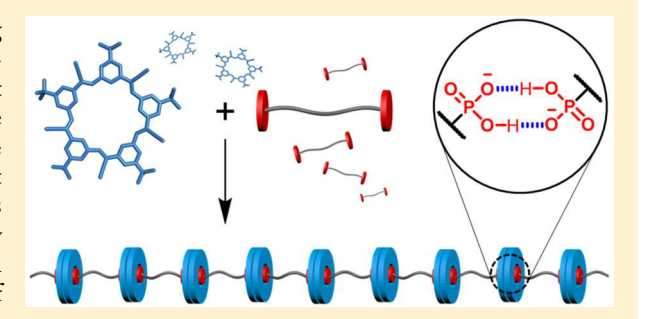


Linear Supramolecular Polymers Driven by Anion-Anion **Dimerization of Difunctional Phosphonate Monomers Inside Cyanostar Macrocycles**

Wei Zhao, Bo Qiao, Joshua Tropp, Maren Pink, Jason D. Azoulay, and Amar H. Flood*,

Supporting Information

ABSTRACT: Supramolecular polymers have enabled far-reaching fundamental science and the development of diverse macromolecular technologies owing to the reversible and noncovalent chemical connectivities that define their properties. Despite the unabated development of these materials using highly tailorable recognition elements, anion-based polymers remain rare as a result of the weak interactions they mediate. Here, we use design rules inspired by cation-driven polymers to demonstrate a new noncovalent link based on receptor-stabilized anion-anion interactions that enables the efficient linear polymerization of simple difunctional phosphonates. The linear main chain



connectivity and molecular topology were confirmed by single crystal X-ray diffraction, which demonstrates the rare 2:2 stoichiometry between the anionic phosphonate end groups and a pair of π -stacked cyanostar macrocycles. The stability of these links enables rapid polymerization of difunctional phosphonates employing different aliphatic linkers (C₆H₁₂, C₈H₁₆, C₁₀H₂₀, C₁₂H₂₄). Diphosphonates with greater chain flexibility (C₁₂H₂₄) enable greater polymerization with an average degree of polymerization of nine emerging at 10 mM. Viscosity measurements show a transition from oligomers to polymers at the critical polymerization concentration of 5 mM. In a rare correlation, NMR spectroscopy shows a coincident molecular signature of the polymerization at 5 mM. These polymers are highly concentration dependent, reversibly polymerize with acid and base, and respond to competitive anions. They display the design simplicity of metallo-supramolecular polymers with transfer of the strong 2:2 recognition chemistry to macromolecules. The simplicity and understanding of this new class of supramolecular polymer is anticipated to open opportunities in tailoring anion-based functional materials.

INTRODUCTION

Supramolecular polymers are of interest for their unique mechanical, 1,2 self-healing, 3,4 and dynamically tunable properties. 5,6 To establish the design rules that govern the properties and functionality of these materials, a variety of recognition elements have been translated into diverse difunctional monomers enabling their supramolecular polymerization. In principle, any noncovalent interaction that is sufficiently strong can be employed,⁷ and many classes of interactions, e.g., hydrogen bonding,⁸ π stacking,^{9,10} and cation coordination, 3,11-13 have been translated into supramolecular polymers. In the case of transition metals³ the design space is elegantly simple. Strong, dependable, and structurally well-defined coordination geometries that form around inorganic cations define 2:1 recognition stoichiometries between two ligands and one ion. The two ligands are then fashioned into the reactive ends of difunctional monomers that polymerize upon addition of metal cations to form linear topologies in which the original 2:1 recognition element lives on inside the polymer (Figure 1a). Anions have the appearance of being like cations but with

negative charges and are therefore expected to spawn similar strategies. However, anions account for little more than two dozen of the 10 000 reports associated with supramolecular polymers. 14 The intrinsic low stability of anion interactions 15 complicates the efficient linear polymerization of even simple monomers and precludes an understanding of how the fundamental properties of anion recognition manifest in supramolecular/macromolecular systems and potential applications. 16,17 Efforts to access stronger anion binding usually rely on the use of large chelating receptors or macrocycles. Being large, their steric profile prevents a second receptor from engaging and inhibits the higher-order 2:1 stoichiometry typically used in simple linear polymerization of difunctional monomers. Thus, there remains a need to combine strong binding with higher order recognition stoichiometries to extend the design simplicity of cation-driven supramolecular polymers to anions (Figure 1b).

Received: January 8, 2019 Published: February 21, 2019



[†]Department of Chemistry, Indiana University, 800 East Kirkwood Avenue, Bloomington, Indiana 47405, United States [‡]School of Polymer Science and Engineering, The University of Southern Mississippi, 118 College Drive, Hattiesburg, Mississippi 39406, United States

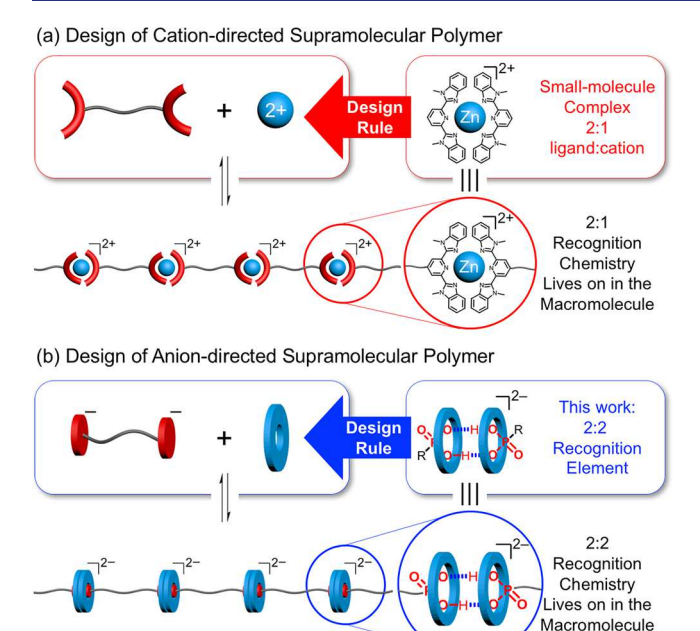


Figure 1. Design space for linear supramolecular polymerization is based on small-molecule recognition elements: (a) metallo-supramolecular polymers formed with a 2:1 ligand:ion linkage stoichiometry (prior work), and (b) an anion-directed supramolecular polymer based on a 2:2 macrocycle:anion linkage stoichiometry (this work).

The first strategies to create anion-driven supramolecular polymers ¹⁸ pioneered by Sessler ¹⁹ made use of copolymers with pendant anion receptors, e.g., calixpyrroles, ²⁰ aryltriazoles, ²¹ aryl-triazoliums, ²² and ion-pair receptors. ^{19,23} These materials were used in the sensing and extraction of inorganic anions, ^{19–21} demonstrations of self-healing, ²² and concentration-driven changes in viscosity and gelation. ²⁴ A second approach investigated by Taylor ^{25,26} and others ^{27,28} involved creation of polymers with anion-stabilizing moieties, e.g., squaramides ^{25,26} or aryl-triazoles, ^{27,28} embedded within the main chain to facilitate anion-driven gelation. These early approaches demonstrated how anion-driven supramolecular polymers could be made using cross-linked topologies.

Linear topologies have also been explored by using various difunctional monomers. The first involved a new class of cationic macrocycle called "Texas-sized" boxes that stabilized either acid-anion linkages inside the macrocycles using terephthalate²⁹ or anion-cation interactions with the naphthalenedicarboxylate dianion.³⁰ Other examples featured linear polymerization between dicationic porphyrins and dianionic difunctional sulfonates,³¹ and between cationic triazolium units^{22,32} that polymerize with either anionic phosphate or carboxylate. The recognition elements in these polymers benefit from stabilizing ionic interactions. There are two examples of linear polymerization without anion-cation contacts. The first features custom-built heterodifunctional buckyball-carboxylates that polymerize with calixpyrrole-based macrocycles.³³ The second involves polymerization of a headto-tail monomer composed of a calixpyrrole macrocycle functionalized with carboxylate.34

Parallel with using different polymer topologies to understand and establish the design rules of anion-driven supramolecular polymers are the insights offered by detailed characterization. Across the existing examples, crystal structures are common^{29–32,35–38} and help to reveal the identity of

the possible noncovalent contacts. However, these interactions do not always directly translate to solution³⁴ precluding fundamental investigations of anion recognition in these systems. Understanding the driving forces of supramolecular polymerization requires solution studies. Concentration-driven changes in average polymer size have been seen by dynamic light scattering (DLS), 25,32,33 by viscosity with the emergence of a critical polymerization concentration (CPC), 24,34,39 and in the form of anion-triggered gelation. 24,25,28 These behaviors are diagnostic of the macromolecular character of the materials created. It is rare, however, to correlate these polymer properties to the molecular-level signatures of the recognition element responsible for driving the polymerization. These correlations offer access to deeper insight. 7,8,40,41 We found one case³² involving anions where the NMR signature was correlated to the extent of polymerization between cationic triazolium and sulfates. However, without a small-molecule analogue, it was not possible to use knowledge of the recognition element to help understand the polymerization. Direct spectroscopic evidence of the recognition element that drives polymerization, which helps enable deeper understanding, remains outstanding in anion-driven supramolecular polymers.

Inspired by the design rules used with metallo-supramolecular polymers, we show a new class of anion-directed polymer where strong, higher-order 2:2 recognition chemistry is used to drive the linear polymerization of simple difunctional monomers. The recognition chemistry $^{42-44}$ involves hydrogenbonded anion—anion dimers of hydroxyanions inside π -stacked dimers of cyanostar macrocycles 45 (Figure 2a). Seen previously with inorganic bisulfate 42,43 and dihydrogen phosphate by

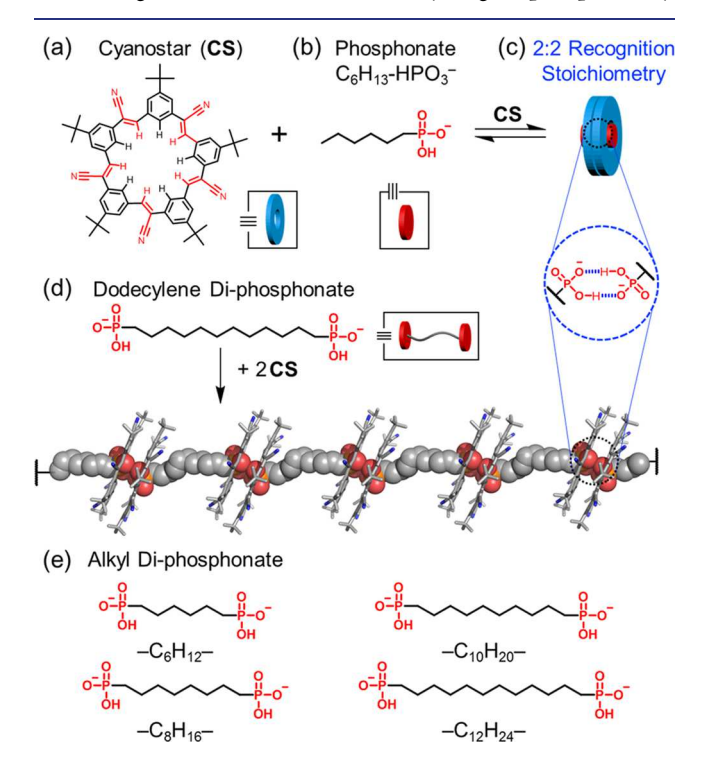


Figure 2. Representations of (a) cyanostar macrocycle, and (b) hexyl monophosphonate (c) that combine together into high-fidelity 2:2 complexes. (d) Difunctional dodecylene diphosphonates undergo dimerization ($-X^-\cdots X^--$) inside cyanostar macrocycles to form supramolecular polymers (crystal structure shown). (e) Structures of alkyl diphosphonate monomers used for polymerization.

us 44,46 and others, 47-49 we extend this recognition element to phosphonate hydroxyanions for the first time (Figure 2c). We present a unique combination of characterizations of the linear polymer spanning from the solid state (Figure 2d) to the solution phase. We describe a rare correlation between the concentration-driven polymerization observed by viscosity to the molecular-level NMR signature of polymerization. This correlation provides direct evidence that conversion of oligomers into large linear polymers results from the 2:2 recognition element: The behavior of the anion-based small molecule lives on inside the macromolecule to drive polymerization. Continuing with this transfer of function, we show that the acid-base switching seen in small molecules⁵⁰ also translates to the reversible and cyclical switching between polymer and small molecule. The reliable transfer of the recognition chemistry from a small molecule to a polymer has much in common with metallo-supramolecular polymers and bodes well for helping establish the design rules governing the structures and properties of anion-driven supramolecular polymers.

■ RESULTS AND DISCUSSION

Molecular Design. The design rules employed herein are based on linear metallo-supramolecular polymers and cation coordination. This begins with selecting a simple, strong recognition element that displays a higher order stoichiometry in a small-molecule complex, e.g., 2:1. Take the component present at the higher molar ratio (i.e., 2) and convert it into a difunctional monomer, and then add the other component to drive linear polymerization. In this way, we expect the recognition element present in the small molecule to live on inside the polymer (Figure 1).

To test the transferability of these design rules, we are using a new noncovalent link based on receptor-stabilized anion—anion interactions. $^{42-44,46-48,50}$ Despite the expectation that the anion—anion linkage is unstable on electrostatic grounds, it is surprisingly strong. This recognition motif relies on the discovery that hydroxyanions $(-X^-)$, like bisulfate 42,43 and dihydrogen phosphate, 44,50 can form homodimers stabilized by a pair of strong and self-complementary OH···O⁻ hydrogen bonds inside a stacked pair of macrocyclic cyanostar receptors. The strength of these supramolecular links has been quantified in the assembly between two bisulfate anions and two cyanostars in a 2:2 stoichiometry at $\Delta G = -96$ kJ mol⁻¹ $(\beta_{2:2} \sim 10^{17} \text{ M}^{-3}, \text{CH}_2\text{Cl}_2)$.

We also needed to consider that anion—anion interactions and the 2:2 stoichiometry^{51–53} offer new types of reversible and noncovalent chemical connectivities, molecular topologies and functionality. The 2:2 stoichiometry is rare^{51–53} when considered next to the prevalence of 1:1 stoichiometries with hydrogen-bonded supramolecular polymers⁸ and 2:1 (or 3:1) stoichiometries for cation coordination.^{11,12} Such 2:2 linkages may be expected to confer higher entropic penalties and a greater concentration dependence arising from the coming together of four components relative to 1:1 and 2:1 stoichiometries. Nevertheless, we hypothesize that the stability is sufficient to offset any entropic penalties of polymerization.

When considering the opportunities of the 2:2 recognition stoichiometry, and by applying the design rules seen with metallo-supramolecular polymers (vide supra), we have the freedom to create difunctional monomers with end groups composed of either two macrocycles or two anions. We pursued the latter on account of their simplicity and

modularity. On the basis of the well-established anion-binding profile of cyanostar, ^{42,45} we needed hydroxyanions that were size-complementary to the macrocycle's binding pocket. Commercially available diphosphonic acids with various alkyl linkers enabled relatively quick access to a variety of diphosphonate monomers by ionization to test their polymerization in the presence of cyanostars.

2:2 Cyanostar:Phosphonate Linkages in Model Complexes. We started by evaluating if the known 2:2 binding stoichiometry⁵⁰ between cyanostar and phosphate hydroxyanions can be retained with phosphonate hydroxyanions by using a model monofunctional compound. Hexyl monophosphonate $(C_6H_{13}-HPO_3^-)$ was prepared by deprotonation of the corresponding acid using tetrabutylammonium hydroxide (TBAOH). NMR titrations, 2D NMR experiments (gCOSY, NOESY, Figures S4–S5) and diffusion NMR (Figure S20) are fully consistent with formation of a high-fidelity 2:2 complex. Starting from the four-line pattern of cyanostar (Figure 3a), 1 equiv of $C_6H_{13}-HPO_3^-$ produces the signature

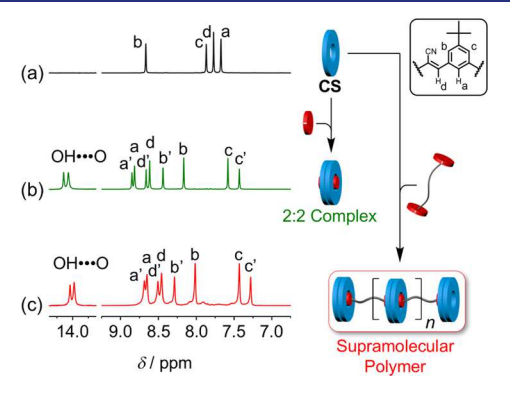


Figure 3. 1 H NMR spectra of (a) free cyanostar macrocycle (5 mM, CD₂Cl₂, 298 K, 600 MHz), with either (b) 1.0 equiv of hexyl monophosphonate (C_6H_{13} -HPO₃ $^{-}$), or (c) 0.5 equiv of dodecylene diphosphonate ($^{-}$ HPO₃ $^{-}$ Cl₂H₂₄-HPO₃ $^{-}$).

of the 2:2 complex (green trace, Figure 3b). First, the pair of aromatic peaks around 7.5 ppm assigned to protons c and c' are diagnostic of π -stacked cyanostar dimers on account of the fact that they only emerge when two pro-chiral cyanostar macrocycles come together to form *meso* and *chiral* diastereomeric combinations. Consistently, all the aromatic protons show diastereomers. The splitting in the phosphorus signals assigned to the diphosphonates in the ³¹P NMR spectra also correspond to these diastereomers (Figure S13). Second, the highly downfield shifted 14-ppm peaks that are indicative of strong hydrogen bonding 4 verifies the dimerization of the phosphonate anions. This 2:2 NMR signature of the anion dimer inside the stacked cyanostar dimers is expected to be reproduced if this recognition element remains in the polymers.

Fortuitously, the NMR spectra of the model complex only show the 2:2 recognition stoichiometry. We did not observe evidence for the 2:1 or 3:2 complexes seen with other hydroxyanions. We have previously shown that steric groups on organophosphates are required to favor the 2:2 stoichiometry. Presumably, the phosphonate's α methylene group (P-CH₂-) introduces sufficient steric pressure to favor the 2:2 species over a triple-stacked 3:2 complex. The high-fidelity production of the 2:2 species greatly simplifies the NMR spectra, and thus the subsequent analyses to allow the

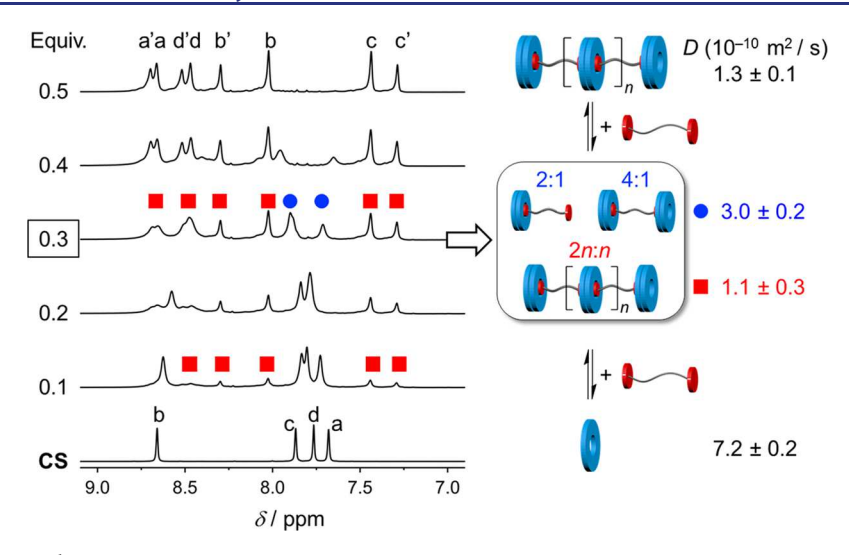


Figure 4. Titration showing the ¹H NMR spectra of cyanostar (10 mM, CD₂Cl₂, 298 K, 600 MHz) upon addition of dodecylene diphosphonate, with the proposed species and measured diffusion coefficients (*D*) shown on the right (red square, supramolecular polymer; blue circle, oligomer).

properties of the resulting macromolecules to be related to a single recognition element.

The first benefit of the simplified analysis is in the estimation of the stability of the 2:2 complex at -83 ± 3 kJ mol $^{-1}$ ($\beta_{2:2} \approx 10^{14.5}$ M $^{-3}$, CH $_2$ Cl $_2$) based on competition titrations conducted with perchlorate, $\beta_{2:1}$ (ClO $_4$ $^-$) = 10^{12} M $^{-2}$ (Figure S10). The stability of the model 2:2 complex serves as a benchmark for evaluating if the strength of this recognition chemistry can be used to drive polymerization.

Preparation of the Linear Supramolecular Polymer. We evaluated the supramolecular polymerization using the difunctional monomer dodecylene diphosphonate ($^{-}$ HPO $_{3}^{-}$ C $_{12}H_{24}$ –HPO $_{3}^{-}$) as a TBA $^{+}$ salt. Addition of 0.5 equiv of the diphosphonate to cyanostar provides the ideal ratio needed for polymerization. The resulting 1 H NMR spectrum (red trace, Figure 3c) displays all the characteristics of the 2:2 complex (Figure 3b) indicating that the recognition chemistry persists in the polymer. We see the same diastereomeric protons in the aromatic region and the same hydrogen bonding signal at 14 ppm (Figure 3c). 2D NMR experiments are also consistent with this assignment (Figures S6–S7). The titration data (Figure 4) shows that the clean 1 H NMR spectrum of the polymer only occurs when the right stoichiometry exists between cyanostar and the diphosphonate (2:1 molar ratio).

The titration data (Figure 4) provides signatures of the various complexes that are present at the substoichiometric ratios leading to the polymer. Upon addition of just 0.1 equiv of the diphosphonate monomer to the cyanostar, we instantly see peaks (red squares, Figure 4) belonging to the polymer, e.g., protons c and c' at \sim 7.4 ppm. With further addition of the monomer (0.1-0.4 equiv), we see the cluster of peaks at 7.8 ppm. These peaks display behavior that is characteristic of a 2:1 complexation event between two cyanostar macrocycles and just one of the two phosphonate end groups of the difunctional monomers. This type of signature has been seen in many titrations 42–44,50 between cyanostar and various anions with the same smooth shifts upfield (protons b and c) and downfield (protons a and d). The main difference to those small-molecule examples is the loss in intensity concomitant with growth in the peaks for the supramolecular polymer.

Diffusion NMR experiments clearly distinguish the oligomers from the polymers. For instance, at 0.3 equiv of

added diphosphonate monomer, protons assigned to the polymer produce a diffusion coefficient of $1.1 \pm 0.3 \times 10^{-10}$ m²/s. This value matches the one measured from the supramolecular polymer ($1.3 \pm 0.1 \times 10^{-10}$ m²/s) present with the ideal 0.5 equiv of diphosphonate. In contrast, the protons assigned to the oligomer around 7.8 ppm have a much higher diffusion coefficient of $3.0 \pm 0.2 \times 10^{-10}$ m²/s consistent with a species that is smaller than the polymer.

Taken together, the NMR signatures of the oligomers seen in the substoichiometric region of the titration report the presence of 2:1 complexation events. These could occur at just one or both ends of the difunctional monomer generating a final 2:1 or 4:1 ratio of cyanostar to monomer (see cartoon representation at 0.3 equiv in Figure 4). It is likely that both species are present during the titration. It is also possible that these signatures represent end groups of the growing linear polymer. For example, for a degree of polymerization of two, there might be two 2:1 end groups and one 2:2 supramolecular link (six cyanostar macrocycles and two diphosphonates, n =1). We were also hoping to identify and distinguish different end groups from signals in the aliphatic region of the NMR spectra, e.g., the uncomplexed phosphonate end group in the oligomer with 2:1 stoichiometry. However, peak overlap with the polymer and/or countercation (TBA+) prevented a clear view. Ultimately, the titration data show that oligomers get converted into the polymer at the stoichiometric equivalence point (0.5 equiv).

Single-Crystal X-ray Structure of the Linear Supramolecular Polymer. The formation of supramolecular linkages is clearly established from the crystal structure (Figures 2d and 5). Despite disorder in the dodecyl chains and the whole-molecule disorder typical of cyanostar, 45,55 the packing of the macrocycles and the diphosphonate monomers is clear. We see phosphonate hydroxyanions dimerized inside π-stacked pairs of macrocycles defining the 2:2 recognition stoichiometry (Figure 5). Two TBA⁺ countercations sit between the repeating macrocycle dimers such that there is no space for an extra macrocycle to generate the triple stacks of cyanostar seen with different hydroxyanions in solution studies. $^{42-44,50}$ The overall 2n:n stoichiometry of the two components agrees with the ideal ratio for the linear supramolecular polymer. The structure also shows hierarchical

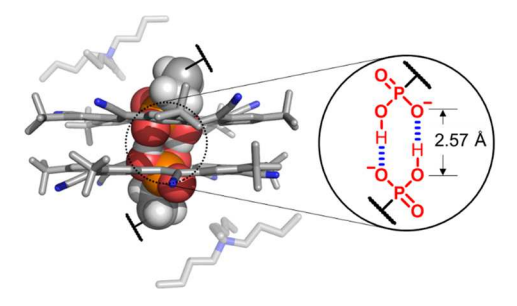


Figure 5. Crystal structure of the supramolecular link at the heart of the polymerization composed of a 2:2 complex of two macrocycles, and two diphosphonates (alkyl chains truncated). This structure also shows the location of the two TBA⁺ cations in solid state.

self-assembly with continuous noncovalent and covalent links running through the solid-state material (Figure 2d) forming the linear supramolecular polymer as designed.

Monomer Modularity. Diphosphonate monomers with shorter linkers (C_6H_{12} , C_8H_{16} , $C_{10}H_{20}$, Figure 2e) were also capable of supramolecular polymerization (Figure S15-S17). The shorter monomers yielded similar results to the dodecylene diphosphonate but with poorer solubility. This observation indicates that greater flexibility in the monomers can confer favorable properties, in this case, for more extensive supramolecular polymerization accessible at higher concentrations. The NMR signatures of the polymers composed of these shorter monomers showed the same patterns but with small shifts in the positions of the cyanostar's aromatic peaks. As the chains get shorter, so too do the distances between repeating cyanostar dimers leading to greater ring current effects between nearest neighbors, and the aromatic peaks are located at progressively upfield locations. Consistent with this idea, the peaks for the polymer made from the C₁₂H₂₄ linker are also shifted upfield (Figure 3) relative to the smallmolecule 2:2 complex, which has no neighboring cyanostar

Concentration-Driven Polymerization. To verify that the NMR signatures and the diffusion coefficients of the 2:2 recognition element correspond to a supramolecular polymerization, concentration-driven studies were undertaken. We first studied changes in specific viscosity (Figure 6a). 8,24 The double-logarithmic plot of specific viscosity versus concentration shows an initial slope (0.32) consistent with noninteracting assemblies of constant size that changes to a value (1.67) indicative of a linear polymer. This changeover occurs at around 5 mM and, on the basis of prior work on supramolecular polymerization, 8,41 it is assigned to the critical polymerization concentration (CPC). The observation of a CPC is diagnostic of concentration-driven polymerization that proceeds readily in solution.

The existence of slow exchange NMR signals for this anion-driven supramolecular polymer is rare, and it provides us with a unique opportunity to investigate the mechanism of polymerization. The variable concentration NMR spectra show a clear correlation to the critical polymerization concentration (Figure 6b). Below the CPC of 5 mM, we see NMR peaks assigned to oligomers (blue circles) and to the polymer (red squares), whereas above 5 mM we only see a single set of peaks for the polymer (red squares). Across the lower concentrations (0.5–5.0 mM), we see that the locations and shifts of the oligomer peaks closely resemble the ones seen in the titration (Figure 4). This correspondence strongly

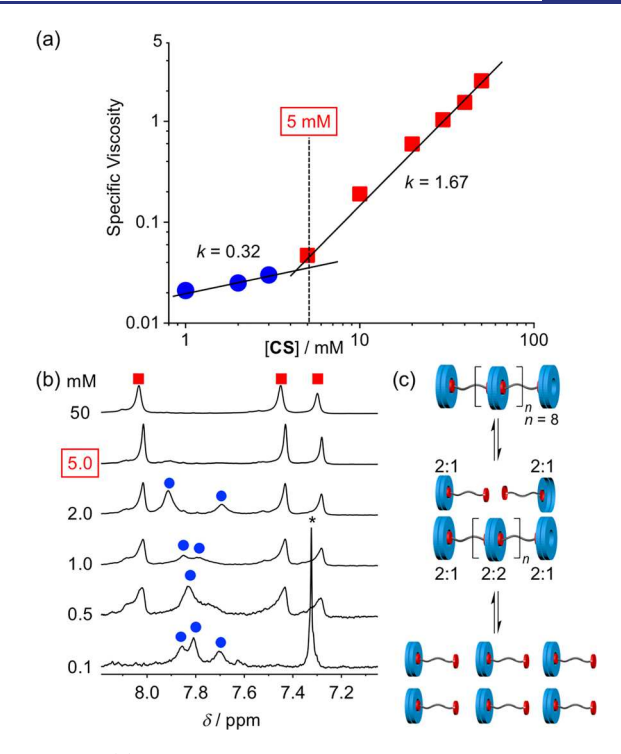


Figure 6. (a) Characterization of polymerization using double logarithmic plots of specific viscosity versus cyanostar concentration with 0.5 equiv of diphosphonate (CHCl₃). (b) Partial ¹H NMR spectra of cyanostar with 0.5 equiv of diphosphonate as a function of concentration (CD₂Cl₂, 298 K, 600 MHz; red square, supramolecular polymer; blue circle, oligomer; * residue CHCl₃ peak). (c) The proposed mechanism of concentration-driven supramolecular polymerization.

suggests the existence of similar 2:1 end groups and oligomers below the CPC. Consistently, the diffusion coefficients derived from the peaks assigned to these oligomers are much larger than for the polymers. For example, at 1 mM the smaller oligomers diffuse more rapidly ($D=4.8\pm0.4\times10^{-10}~\text{m}^2/\text{s}$) relative to the diffusion of the polymers ($D=1.9\pm0.2\times10^{-10}~\text{m}^2/\text{s}$), and a similar situation is seen at 2 mM (3.5 ± 0.3 vs 1.9 ± 0.4 × 10⁻¹⁰ m²/s, respectively).

We also see that the absolute peak intensities of the two sets of peaks are indicative of concentration-driven conversion of oligomer to polymer (Figure 6b). From 0.5 to 50 mM, we see a continuous and linear increase in the peak intensity of the supramolecular polymer (Figure S14). Similar results were seen with other supramolecular polymers. S6,57

We corroborated the concentration-driven polymerization by following increases in the average size of the polymer using dynamic light scattering (Figure 7a). The data show the average hydrodynamic radius grows from 6 to 16 nm with concentration ([CS]: 1 to 50 mM, CH₂Cl₂). We examined the macrocycle alone as a control. While it can self-associate to a small degree, its average size is only 3 nm at 25 mM. The large difference in size (\sim 3 nm vs \sim 16 nm) in the presence of the diphosphonate confirms the diffunctional monomer's role in producing a large macromolecule in solution. Consistently, the diffusion coefficient measured using NMR experiments from the peaks for the polymer show dramatic decrease as the concentration is increased (Figure S24) from 1 mM (2.0 \times 10⁻¹⁰ m²/s) to 50 mM (0.75 \times 10⁻¹⁰ m²/s) indicative of a 19-fold volume change. This volume change perfectly matches the

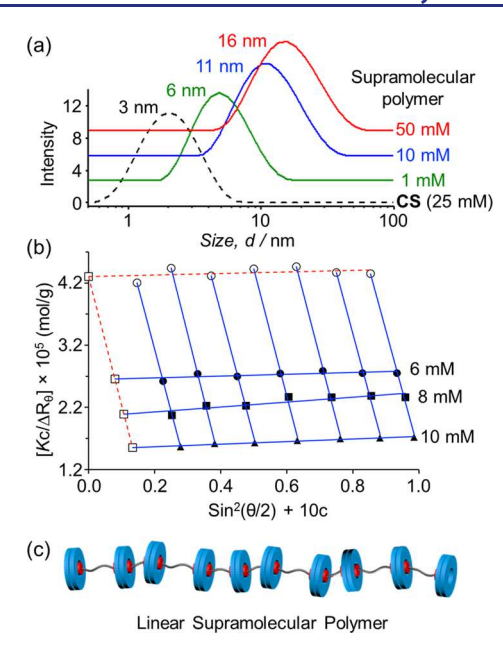


Figure 7. (a) Dynamic light scattering of cyanostar (dashed line, 25 mM), and the supramolecular polymer (2:1, cyanostar:dodecylene diphosphonate) at various macrocycle concentrations (298 K, CH₂Cl₂). (b) Zimm profile acquired from variable-concentration, multiangle light scattering on the supramolecular polymer above the CPC (298 K, CHCl₃, 633 nm). (c) Proposed linear, extended solution structure of the supramolecular polymer (one possible microstate is shown).

19-fold change in volume determined from the DLS experiments.

Given that each of the 2:2 supramolecular linkages has a double negative charge, we investigated the role of ion pairing on the polymerization. We might expect that increased ion pairing would help screen the buildup of negative charge density along the growing polymer chain to enhance the extent of polymerization. To enhance the conditions for the propensity for ion pairing, we repeated our studies in chloroform. Its lower dielectric constant ($\varepsilon = 4.5$) relative to dichloromethane ($\varepsilon = 8.9$) will significantly enhance the pairing between the dianionic 2:2 sites present all along the linear chain and the TBA+ countercations. 58 Despite this change, the NMR signatures, diffusion NMR values, and DLS sizes (Figures S18 and S26) all matched those seen in dichloromethane suggesting little difference in the extent of ion pairing between these solvents. The only distinction was in the ~14 ppm region of the NMR spectra. In addition to the diastereomeric pair of hydrogen bonded OH···O⁻ peaks at ~14 ppm, we see the emergence of a second diastereomeric pair of peaks at ~13.7 ppm that grow in relative intensity with concentration (Figure S19). We attribute these signals to slowexchange ion pairing. Presumably, the ion pairing in dichloromethane is under fast exchange. We also sought to enhance ion pairing by adding excess TBA+. The countercation concentration was raised by adding TBA+ as the salt of the anion tetrakis(3,5-bis(trifluoromethyl)phenyl)borate (BArF⁻), which is too large to bind to cyanostar. At concentrations below the CPC ([CS] = 2 mM, CDCl₃), addition of a 30-fold excess of TBA+ (60 mM) showed no changes to the ratios of the oligomers and the polymers as verified by NMR spectroscopy (Figure S39). The same outcome was observed above the CPC ([CS] = 10 mM) with 5 equiv of TBA⁺ (50 mM). Taken

together, these results suggest that while ion pairing is present in both these solvents, it has little effect on the extent of polymerization under the conditions we examined.

To estimate the average molecular weight of the supramolecular polymer, we conducted multiangle light scattering in chloroform above the CPC using a Zimm plot^{59,60} (Figure 7b). Zimm plots are a conventional approach to characterize polymer sizes using static light scattering experiments acquired over multiple angles and as a function of concentration. Such plots are used occasionally to analyze supramolecular polymers. 41,61 Nevertheless, the applicability of the Zimm plot is seen in the data linearity (Figure 7b) consistent with similar studies on a metallo-supramolecular polymer. 62 The Zimm plot provides a radius of gyration (R_{σ}) for the supramolecular polymer of 12 ± 2 nm at a cyanostar concentration of 10 mM (CHCl₃). This value is consistent with sizes seen by DLS. The weight-average molecular weight $(M_{\rm w})$ was determined to be 23.5 \pm 0.4 kDa indicating an average degree of polymerization (DP) of nine at 10 mM.

Interestingly, the radius of gyration ($R_{\rm g}=12~{\rm nm}$) at 10 mM is about twice as large as the hydrodynamic radius ($R_{\rm h}=5.5~{\rm nm}$) seen from DLS (Figure 7a). The ratio of the two, $R_{\rm g}/R_{\rm h}\sim 2$, suggests that the supramolecular polymer chain tends to be in an extended conformation on average (Figure 7c), 63,64 which is consistent with the solid-state packing (Figure 2d). For comparison, the contour length of a fully extended 1D supramolecular polymer chain with nine repeat units is about 13.6 nm (Figure S44) consistent with $R_{\rm g}$ and $R_{\rm h}$. Sharp peaks in the NMR spectrum (Figure 3c) also suggest a low degree of aggregation of the polymer in solution. All these observations support an extended supramolecular polymer chain.

On the basis of the viscosity measurement, NMR experiments, and the light scattering data, we proposed a mechanism for the concentration-driven supramolecular polymerization (Figure 6c). At low concentrations (<5 mM), we see oligomers and polymers present in solution. Below the CPC, the solution is dominated by oligomers and short polymer chains that diffuse fast and allow the solution to flow freely with low specific viscosity. As the concentration increases, all the oligomers are converted into increasing longer polymer chains. Above the CPC, polymers now dominate in solution. They diffuse more slowly and when the solution is subjected to flow become aggregated thus giving rise to high viscosities.

In some supramolecular polymers that are composed of more flexible monomers, ^{8,41} the CPC has been attributed to the transition from cyclic polymers to linear polymer topologies. An elementary rigid-body molecular model of the macromolecule (Figure S45) shows a pentamer would be the smallest cyclic structure that could be accommodated. However, the NMR spectra below the CPC clearly show the signature for the 2:1 complex (Figure 6b, 0.1–2.0 mM). These 2:1 signatures are representative of end groups instead of the 2:2 signatures that would be required for cyclic structures.

We observed precipitation of the material under certain conditions and, for this reason, all solution studies were conducted either with filtered samples or prior to the onset of precipitation. Consistent with other reports, 29,65 the precipitate forms almost instantaneously at higher concentrations (100 mM in our case) and more slowly at lower concentrations. The precipitate cannot be redissolved in the original solvent (CH₂Cl₂) suggesting that the supramolecular polymer irreversibly aggregates. 65 This interpretation is consistent

with the negative second virial coefficient ($A_2 = -1.008 \pm 0.037 \times 10^{-3} \text{ cm}^3 \text{ mol g}^{-2}$) from the Zimm analysis.⁶⁶

Stimuli-Responsive Properties. To investigate the dynamic character of the supramolecular polymers, we characterized its switchable and stimuli responsive behaviors. First, supramolecular polymerization can be produced by in situ addition of base (TBAOH) to a 2:1 mixture of cyanostar and the premonomer, diphosphonic acid. We used $20:80 \ v/v \ \text{CD}_3\text{CN:CD}_2\text{Cl}_2$ in order to solubilize all the components. Addition of 1.0 equiv of TBAOH relative to diphosphonic acid will produce a single phosphonate anion at one end of the monomer. Consistently, we only see an NMR signature of the 2:1 complex (Figure S28). This 2:1 stoichiometry was verified with the aid of the diffusion coefficient (Figure 8). S0

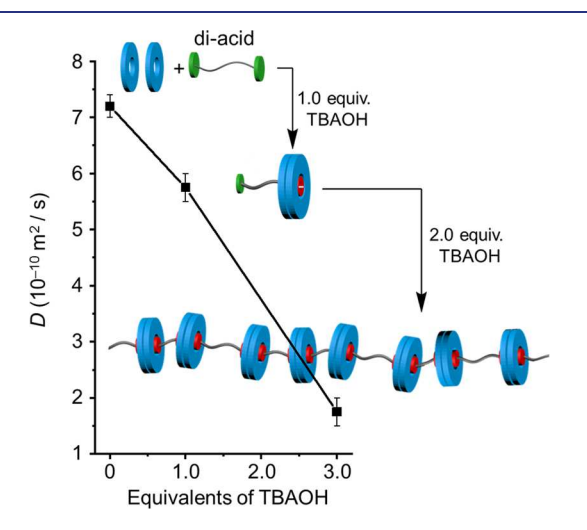


Figure 8. Changes in diffusion coefficient associated with cyanostar macrocycle (5 mM) upon addition of 1 and 3 equiv of tetrabutylammonium hydroxide (298 K, 600 MHz, 20:80 v/v CD₃CN:CD₂Cl₂).

One more equivalent of base fully deprotonates the monomer generating the second phosphonate to drive polymerization in situ with a dramatic drop in diffusivity (Figure 8). The water produced in the acid—base reaction is believed to have a minimal effect on the polymerization based on negligible changes in the NMR spectra of the supramolecular polymer upon addition of 10 equiv of water (Figure S29).

We next tested the capacity for reversible switching of the phosphonate-driven supramolecular polymer using acid and base (Figure 9) and the transfer of function from the smallmolecule to the macromolecule. On the basis of our prior work,⁵⁰ we used picric acid (PA) and 1,8-diazabicyclo[5.4.0]undec-7-ene (DBU) as the acid and base, respectively. Addition of 1.0 equiv of PA to the supramolecular polymer $([CS] = 10 \text{ mM}, 20:80 \text{ v/v } CD_3CN:CD_2Cl_2)$ drives depolymerization. The resulting ¹H NMR spectra of the polymer (black, Figure 9b) is consistent with a noninteracting mixture of the free cyanostar, picrate (green, Figure 9a) and diphosphonic acid. The polymer is recovered upon addition of 2.0 equiv of DBU (Figure 10a) producing a diffusion coefficient (1.4 \pm 0.1 \times 10⁻¹⁰ m²/s) matching the original value (Figure 8). The reversible acid-base interconversion between monomer and supramolecular polymer was verified over four cycles (Figure 10) using ¹H NMR. The diffusion coefficients (Figure 10b) also track with the acid-base driven cycling between small and large molecular weight species. This

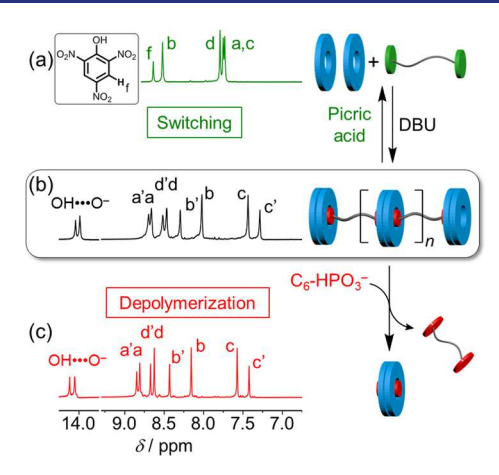


Figure 9. ¹H NMR spectra of (a) supramolecular polymer ([CS] = 10 mM, 298 K, 600 MHz, 20:80 v/v $CD_3CN:CD_2Cl_2$) with 1.0 equiv of picric acid; (b) supramolecular polymer; (c) supramolecular polymer ([CS] = 10 mM, 298 K, 600 MHz, CD_2Cl_2) after addition of 1.0 equiv of hexyl monophosphonate.

transfer of function is consistent with the 2:2 recognition chemistry living on inside the polymer.

The supramolecular polymer also responds to competing anions. Depolymerization can be driven by a variety of anions. We first tried anions known to form 2:1 complexes. Those anions that bind strongest to cyanostar are more effective at depolymerization, $PF_6^- > I^- > Br^- > Cl^-$. Next, we investigated competition with anions forming 2:2 linkages. Addition of just 1.0 equiv of the monofunctional hexyl monophosphonate can also fully disassemble the supramolecular polymer into the discrete 2:2 complexes between cyanostar and C₆H₁₃-HPO₃⁻ (Figure 9c) with the diphosphonates released as free monomers. This observation provides a basis to consider the driving forces operating in this depolymerization. The 2:2 supramolecular linkage in the polymer and the recognition motif in the 2:2 complex are equivalent. Under this condition, we might assume that the enthalpies of interaction are similar. Consequently, we may consider differences in the translational entropy to be the driving force for depolymerization. However, when we consider the hypothetical reaction of one polymer having a degree of polymerization of nine in a reaction with 18 monophosphonates, we produce nine 2:2 complexes and nine difunctional monomers. In this case, the 18 products arise from 19 reactants, which represents a modest change in translational entropy. The depolymerization is therefore attributed to driving forces emerging at the macromolecular level.

CONCLUSIONS

We demonstrated a new anion-driven supramolecular polymer with a linear topology composed of difunctional monomers that follow the design principles common to cation-directed polymers. It is this outcome, and the fact that our recognition system lives on inside the polymer, that allows the polymerization to look straightforward. Yet, this simplicity is remarkable given the rarity of anion-driven supramolecular polymers and the low stability of anion interactions. In this case, a strong reliable recognition element with higher order 2:2 stoichiometry is used as the basis to design a difunctional monomer that readily undergoes polymerization by receptor-assisted anion—anion dimerization using cyanostar macrocycles. We show unambiguous signatures of polymerization, not just in crystals but also in solution, with a rare correlation

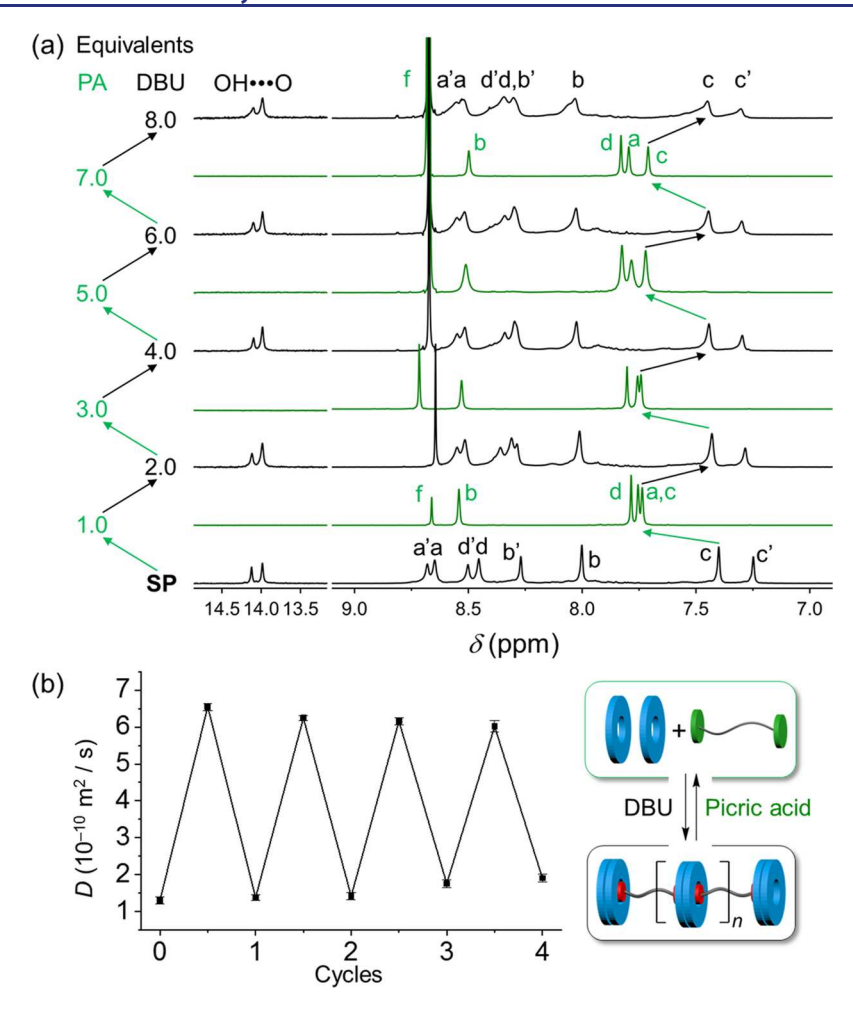


Figure 10. (a) 1 H NMR spectra of the supramolecular polymer composed of cyanostar macrocycle and 0.5 equiv of dodecylene diphosphonates following subsequent additions of picric acid (PA) and DBU base. ([CS] = 10 mM, 20:80 v/v CD₃CN:CD₂Cl₂, 298 K, 600 MHz. The equivalents of PA and DBU are relative to the concentration of the cyanostar macrocycles). (b) Diffusion coefficients change following the repeated acid—base switching of the supramolecular polymer. The diffusion coefficients were determined by averaging values from protons H_a , H_d , H_b and H_c on the macrocycles.

between the concentration-driven change in solution viscosity occurring at the same concentration that we see a clear molecular signature of polymerization by NMR. We show that the original recognition element lives on inside the polymer as based on the NMR signature and the stimuli-responsive behavior. We see that polymerization is switchable under acid—base control and can be irreversibly depolymerized with a competitive anion. This study is the first of its kind that overcomes significant and historically rooted challenges associated with these anion-templated materials, provides detailed mechanistic insight, and opens access to a broad variety of technologically relevant applications thought of as beyond the current scope of anion-driven supramolecular polymer systems.

ASSOCIATED CONTENT

S Supporting Information

The Supporting Information is available free of charge on the ACS Publications website at DOI: 10.1021/jacs.9b00248.

General methods, crystallography, 1D and 2D NMR, diffusion NMR, viscosity measurement, dynamic light scattering and static light scattering data (PDF)

Crystal data (CIF)

AUTHOR INFORMATION

Corresponding Author

*aflood@indiana.edu

ORCID ®

Jason D. Azoulay: 0000-0003-0138-5961 Amar H. Flood: 0000-0002-2764-9155

Present Address

§B.Q.: Research Laboratory of Electronics, Massachusetts Institute of Technology, Cambridge, Massachusetts 02139, United States.

Notes

The authors declare no competing financial interest.

ACKNOWLEDGMENTS

AHF acknowledges support from the National Science Foundation (CHE 1709909). JT and JDA acknowledge support from the National Science Foundation (OIA 1632825). We thank the IU Nanoscale Characterization Facility for access to the Zetasizer for dynamic light scattering experiments.

REFERENCES

- (1) Aida, T.; Meijer, E. W.; Stupp, S. I. Functional supramolecular polymers. *Science* **2012**, *335*, 813.
- (2) Liu, J.; Tan, C. S. Y.; Yu, Z.; Li, N.; Abell, C.; Scherman, O. A. Tough Supramolecular Polymer Networks with Extreme Stretchability and Fast Room-Temperature Self-Healing. *Adv. Mater.* **2017**, *29*, 1605325.
- (3) Burnworth, M.; Tang, L.; Kumpfer, J. R.; Duncan, A. J.; Beyer, F. L.; Fiore, G. L.; Rowan, S. J.; Weder, C. Optically healable supramolecular polymers. *Nature* **2011**, *472*, 334.
- (4) Li, C.-H.; Wang, C.; Keplinger, C.; Zuo, J.-L.; Jin, L.; Sun, Y.; Zheng, P.; Cao, Y.; Lissel, F.; Linder, C.; You, X.-Z.; Bao, Z. A highly stretchable autonomous self-healing elastomer. *Nat. Chem.* **2016**, *8*, 618.
- (5) Chen, H.; Huang, Z.; Wu, H.; Xu, J.-F.; Zhang, X. Supramolecular Polymerization Controlled through Kinetic Trapping. *Angew. Chem., Int. Ed.* **2017**, *56*, 16575.
- (6) Venkata Rao, K.; Miyajima, D.; Nihonyanagi, A.; Aida, T. Thermally bisignate supramolecular polymerization. *Nat. Chem.* **2017**, *9*, 1133.
- (7) Brunsveld, L.; Folmer, B. J. B.; Meijer, E. W.; Sijbesma, R. P. Supramolecular polymers. *Chem. Rev.* **2001**, *101*, 4071.
- (8) Scherman, O. A.; Ligthart, G. B. W.; Sijbesma, R. P.; Meijer, E. W. A Selectivity-Driven Supramolecular Polymerization of an AB Monomer. *Angew. Chem., Int. Ed.* **2006**, *45*, 2072.
- (9) Ogi, S.; Sugiyasu, K.; Manna, S.; Samitsu, S.; Takeuchi, M. Living supramolecular polymerization realized through a biomimetic approach. *Nat. Chem.* **2014**, *6*, 188.
- (10) Weingarten, A. S.; Kazantsev, R. V.; Palmer, L. C.; McClendon, M.; Koltonow, A. R.; Samuel, A. P.; Kiebala, D. J.; Wasielewski, M. R.; Stupp, S. I. Self-assembling hydrogel scaffolds for photocatalytic hydrogen production. *Nat. Chem.* **2014**, *6*, 964.
- (11) Hofmeier, H.; Hoogenboom, R.; Wouters, M. E.; Schubert, U. S. High molecular weight supramolecular polymers containing both terpyridine metal complexes and ureidopyrimidinone quadruple hydrogen-bonding units in the main chain. J. Am. Chem. Soc. 2005, 127, 2913.
- (12) Yount, W. C.; Loveless, D. M.; Craig, S. L. Strong means slow: dynamic contributions to the bulk mechanical properties of supramolecular networks. *Angew. Chem., Int. Ed.* **2005**, 44, 2746.
- (13) Yan, X.; Xu, J.-F.; Cook, T. R.; Huang, F.; Yang, Q.-Z.; Tung, C.-H.; Stang, P. J. Photoinduced transformations of stiff-stilbene-based discrete metallacycles to metallosupramolecular polymers. *Proc. Natl. Acad. Sci. U. S. A.* **2014**, *111*, 8717.
- (14) Literature search was based on the keywords "anion-directed supramolecular polymer" in Web of Science.
- (15) Sessler, J. L.; Gale, P. A.; Cho, W.-S. Anion Receptor Chemistry; Royal Society of Chemistry, 2006; Vol. 8.
- (16) Rambo, B. M.; Silver, E. S.; Bielawski, C. W.; Sessler, J. L. Covalent Polymers Containing Discrete Heterocyclic Anion Receptors. In *Anion Recognition in Supramolecular Chemistry*; Gale, P. A., Dehaen, W., Eds.; Springer: Berlin, Heidelberg, 2010; pp 1.
- (17) Jiang, J.; Zhao, Y.; Yaghi, O. M. Covalent chemistry beyond molecules. J. Am. Chem. Soc. 2016, 138, 3255.
- (18) (a) Prior to Sessler, there were accounts of anion-responsive supramolecular polymers, but they did not derive from anion-driven cross-links. One class was anion-modulated supramolecular polymers with ionic interactions: (b) Kim, H.-J.; Zin, W.-C.; Lee, M. Anion-directed self-assembly of coordination polymer into tunable secondary structure. J. Am. Chem. Soc. 2004, 126, 7009. (c) Applegarth, L.; Clark, N.; Richardson, A. C.; Parker, A. D. M.; Radosavljevic-Evans, I.; Goeta, A. E.; Howard, J. A. K.; Steed, J. W. Modular nanometer-scale structuring of gel fibres by sequential self-organization. Chem. Commun. 2005, 5423. Another class was based on hydrogen bonding: (d) Maeda, H.; Haketa, Y.; Nakanishi, T. Aryl-substituted C3-bridged oligopyrroles as anion receptors for formation of supramolecular organogels. J. Am. Chem. Soc. 2007, 129, 13661. (e) Yamanaka, M.; Nakamura, T.; Nakagawa, T.; Itagaki, H. Reversible sol—gel transition of a tris—urea gelator that responds to chemical stimuli. Tetrahedron

- Lett. 2007, 48, 8990. (f) Byrne, P.; Lloyd, G. O.; Anderson, K. M.; Clarke, N.; Steed, J. W. Anion hydrogen bond effects in the formation of planar or quintuple helical coordination polymers. Chem. Commun. 2008, 3720. (g) Maeda, H. Anion-Responsive Supramolecular Gels. Chem. Eur. J. 2008, 14, 11274.
- (19) Aydogan, A.; Coady, D. J.; Kim, S. K.; Akar, A.; Bielawski, C. W.; Marquez, M.; Sessler, J. L. Poly (methyl methacrylate) s with pendant calixpyrroles and crown ethers: polymeric extractants for potassium halides. *Angew. Chem., Int. Ed.* **2008**, *47*, 9648.
- (20) Aydogan, A.; Coady, D. J.; Lynch, V. M.; Akar, A.; Marquez, M.; Bielawski, C. W.; Sessler, J. L. Poly(methyl methacrylate)s with pendant calixpyrroles: polymeric extractants for halide anion salts. *Chem. Commun.* 2008, 1455.
- (21) McDonald, K. P.; Qiao, B.; Twum, E. B.; Lee, S.; Gamache, P. J.; Chen, C.-H.; Yi, Y.; Flood, A. H. Quantifying chloride binding and salt extraction with poly(methyl methacrylate) copolymers bearing aryl-triazoles as anion receptor side chains. *Chem. Commun.* **2014**, *50*, 13285.
- (22) Tepper, R.; Bode, S.; Geitner, R.; Jäger, M.; Görls, H.; Vitz, J.; Dietzek, B.; Schmitt, M.; Popp, J.; Hager, M. D.; Schubert, U. S. Polymeric Halogen-Bond-Based Donor Systems Showing Self-Healing Behavior in Thin Films. *Angew. Chem., Int. Ed.* **2017**, *56*, 4047.
- (23) Romanski, J.; Piątek, P. Tuning the binding properties of a new heteroditopic salt receptor through embedding in a polymeric system. *Chem. Commun.* **2012**, *48*, 11346.
- (24) Silver, E. S.; Rambo, B. M.; Bielawski, C. W.; Sessler, J. L. Reversible Anion-Induced Cross-Linking of Well-Defined Calix [4] pyrrole-Containing Copolymers. *J. Am. Chem. Soc.* **2014**, *136*, 2252.
- (25) Rostami, A.; Wei, C. J.; Guérin, G.; Taylor, M. S. Anion Detection by a Fluorescent Poly (squaramide): Self-Assembly of Anion-Binding Sites by Polymer Aggregation. *Angew. Chem., Int. Ed.* **2011**, *50*, 2059.
- (26) Rostami, A.; Guérin, G.; Taylor, M. S. Structure—Activity Relationships for Anion-Responsive Poly (squaramides): Support for an Analyte-Induced Noncovalent Polymer Cross-Linking Mechanism. *Macromolecules* **2013**, *46*, 6439.
- (27) Yim, S.-L.; Chow, H.-F.; Chan, M.-C. Transition from low molecular weight non-gelating oligo(amide-triazole)s to a restorable, halide-responsive poly(amide-triazole) supramolecular gel. *Chem. Commun.* **2014**, *50*, 3064.
- (28) Yang, C.; Wu, B.; Chen, Y.; Zhang, K. Gels based on anion recognition between triurea receptor and phosphate anion. *Macromol. Rapid Commun.* **2015**, 36, 750.
- (29) Gong, H.-Y.; Rambo, B. M.; Karnas, E.; Lynch, V. M.; Sessler, J. L. A 'Texas-sized'molecular box that forms an anion-induced supramolecular necklace. *Nat. Chem.* **2010**, *2*, 406.
- (30) Gong, H.-Y.; Rambo, B. M.; Lynch, V. M.; Keller, K. M.; Sessler, J. L. Texas-Sized" Molecular Boxes: Building Blocks for the Construction of Anion-Induced Supramolecular Species via Self-Assembly. *J. Am. Chem. Soc.* **2013**, *135*, 6330.
- (31) Zhang, Z.; Kim, D. S.; Lin, C.-Y.; Zhang, H.; Lammer, A. D.; Lynch, V. M.; Popov, I.; Miljanic', O. S.; Anslyn, E. V.; Sessler, J. L. Expanded porphyrin-anion supramolecular assemblies: environmentally responsive sensors for organic solvents and anions. *J. Am. Chem. Soc.* 2015, 137, 7769.
- (32) Zapata, F.; González, L.; Caballero, A.; Bastida, A.; Bautista, D.; Molina, P. Interlocked Supramolecular Polymers Created by Combination of Halogen- and Hydrogen-Bonding Interactions through Anion-Template Self-Assembly. *J. Am. Chem. Soc.* **2018**, 140, 2041.
- (33) Kim, D. S.; Chang, J.; Leem, S.; Park, J. S.; Thordarson, P.; Sessler, J. L. Redox-and pH-Responsive Orthogonal Supramolecular Self-Assembly: An Ensemble Displaying Molecular Switching Characteristics. *J. Am. Chem. Soc.* **2015**, *137*, 16038.
- (34) Amharar, S.; Yuvayapan, S.; Aydogan, A. A thermoresponsive supramolecular polymer gel from a heteroditopic calix [4] pyrrole. *Chem. Commun.* **2018**, *54*, 829.
- (35) Gale, P. A.; Navakhun, K.; Camiolo, S.; Light, M. E.; Hursthouse, M. B. Anion-anion assembly: A new class of anionic

- supramolecular polymer containing 3, 4-dichloro-2, 5-diamido-substituted pyrrole anion dimers. J. Am. Chem. Soc. 2002, 124, 11228.
- (36) Wang, T.; Yan, X. P. Pyrazino [2.3-g] quinoxaline-Bridged Indole-Based Building Blocks: Design, Synthesis, Anion-Binding Properties, and Phosphate-Directed Assembly in the Solid State. *Chem. Eur. J.* **2010**, *16*, 4639.
- (37) White, N. G.; Carta, V.; MacLachlan, M. J. Layered 2D Sheetlike Supramolecular Polymers Formed by O-H··· Anion Hydrogen Bonds. *Cryst. Growth Des.* **2015**, *15*, 1540.
- (38) White, N. G.; MacLachlan, M. J. Anion and Cation Effects on Anion-Templated Assembly of Tetrahydroxytriptycene. *Cryst. Growth Des.* **2015**, *15*, 5629.
- (39) Zhan, T.-G.; Zhou, T.-Y.; Qi, Q.-Y.; Wu, J.; Li, G.-Y.; Zhao, X. The construction of supramolecular polymers through anion bridging: from frustrated hydrogen-bonding networks to well-ordered linear arrays. *Polym. Chem.* **2015**, *6*, 7586.
- (40) Sijbesma, R. P.; Beijer, F. H.; Brunsveld, L.; Folmer, B. J.; Hirschberg, J. K.; Lange, R. F.; Lowe, J. K.; Meijer, E. Reversible polymers formed from self-complementary monomers using quadruple hydrogen bonding. *Science* **1997**, 278, 1601.
- (41) Liu, Y.; Wang, Z.; Zhang, X. Characterization of supramolecular polymers. *Chem. Soc. Rev.* **2012**, *41*, 5922.
- (42) Fatila, E. M.; Twum, E. B.; Sengupta, A.; Pink, M.; Karty, J. A.; Raghavachari, K.; Flood, A. H. Anions Stabilize Each Other inside Macrocyclic Hosts. *Angew. Chem., Int. Ed.* **2016**, *55*, 14057.
- (43) Fatila, E. M.; Twum, E. B.; Karty, J. A.; Flood, A. H. Ion-pairing and Co-facial Stacking Drive High-fidelity Bisulfate Assembly with Cyanostar Macrocyclic Hosts. *Chem. Eur. J.* **2017**, 23, 10652.
- (44) Fatila, E. M.; Pink, M.; Twum, E. B.; Karty, J. A.; Flood, A. H. Phosphate-phosphate oligomerization drives higher order co-assemblies with stacks of cyanostar macrocycles. *Chem. Sci.* **2018**, *9*, 2863
- (45) Lee, S.; Chen, C.-H.; Flood, A. H. A pentagonal cyanostar macrocycle with cyanostilbene CH donors binds anions and forms dialkylphosphate [3] rotaxanes. *Nat. Chem.* **2013**, *5*, 704.
- (46) Dobscha, J. R.; Debnath, S.; Fadler, R. E.; Fatila, E. M.; Pink, M.; Raghavachari, K.; Flood, A. H. Host-host Interactions Control Self-assembly and Switching of Triple and Double Decker Stacks of Tricarbazole Macrocycles Co-assembled with Anti-electrostatic Bisulfate Dimers. *Chem. Eur. J.* **2018**, 24, 9841.
- (47) He, Q.; Kelliher, M.; Bähring, S.; Lynch, V. M.; Sessler, J. L. A Bis-calix[4]pyrrole Enzyme Mimic That Constrains Two Oxoanions in Close Proximity. *J. Am. Chem. Soc.* **2017**, *139*, 7140.
- (48) Mungalpara, D.; Valkonen, A.; Rissanen, K.; Kubik, S. Efficient stabilisation of a dihydrogenphosphate tetramer and a dihydrogenpyrophosphate dimer by[space]a cyclic pseudopeptide containing 1,4-disubstituted 1,2,3-triazole moieties. *Chem. Sci.* **2017**, *8*, 6005.
- (49) He, Q.; Tu, P.; Sessler, J. L. Supramolecular Chemistry of Anionic Dimers, Trimers, Tetramers, and Clusters. *Chem.* 2018, 4, 46. (50) Zhao, W.; Qiao, B.; Chen, C. H.; Flood, A. H. High-Fidelity Multistate Switching with Anion-Anion and Acid-Anion Dimers of Organophosphates in Cyanostar Complexes. *Angew. Chem., Int. Ed.* 2017, 56, 13083.
- (51) Raeisi, M.; Kotturi, K.; del Valle, I.; Schulz, J.; Dornblut, P.; Masson, E. Sequence-Specific Self-Assembly of Positive and Negative Monomers with Cucurbit [8] uril Linkers. *J. Am. Chem. Soc.* **2018**, *140*, 3371.
- (52) Yu, Z.; Liu, J.; Tan, C. S. Y.; Scherman, O. A.; Abell, C. Supramolecular Nested Microbeads as Building Blocks for Macroscopic Self-Healing Scaffolds. *Angew. Chem., Int. Ed.* **2018**, *57*, 3079.
- (53) Liu, Y.; Yu, Y.; Gao, J.; Wang, Z.; Zhang, X. Water-soluble supramolecular polymerization driven by multiple host-stabilized charge-transfer interactions. *Angew. Chem., Int. Ed.* **2010**, 49, 6576.
- (54) Jeffrey, G. A.; Jeffrey, G. A. An Introduction to Hydrogen Bonding; Oxford University Press: New York, 1997; Vol. 12.
- (55) Liu, Y.; Singharoy, A.; Mayne, C. G.; Sengupta, A.; Raghavachari, K.; Schulten, K.; Flood, A. H. Flexibility Coexists with Shape-Persistence in Cyanostar Macrocycles. *J. Am. Chem. Soc.* **2016**, *138*, 4843.

- (56) Wang, F.; Zhang, J.; Ding, X.; Dong, S.; Liu, M.; Zheng, B.; Li, S.; Wu, L.; Yu, Y.; Gibson, H. W. Metal coordination mediated reversible conversion between linear and cross-linked supramolecular polymers. *Angew. Chem., Int. Ed.* **2010**, *49*, 1090.
- (57) Dong, S.; Luo, Y.; Yan, X.; Zheng, B.; Ding, X.; Yu, Y.; Ma, Z.; Zhao, Q.; Huang, F. A dual-responsive supramolecular polymer gel formed by crown ether based molecular recognition. *Angew. Chem., Int. Ed.* **2011**, *50*, 1905.
- (58) Liu, Y.; Sengupta, A.; Raghavachari, K.; Flood, A. H. Anion binding in solution: beyond the electrostatic regime. *Chem.* **2017**, *3*, 411.
- (59) Zimm, B. H. Apparatus and methods for measurement and interpretation of the angular variation of light scattering; preliminary results on polystyrene solutions. *J. Chem. Phys.* **1948**, *16*, 1099.
- (60) Wyatt, P. J. Light scattering and the absolute characterization of macromolecules. *Anal. Chim. Acta* **1993**, *272*, 1.
- (61) Knoben, W.; Besseling, N. A.; Cohen Stuart, M. A. Chain stoppers in reversible supramolecular polymer solutions studied by static and dynamic light scattering and osmometry. *Macromolecules* **2006**, *39*, 2643.
- (62) Munzert, S. M.; Schwarz, G.; Kurth, D. G. Tailoring length and viscosity of dynamic metallo-supramolecular polymers in solution. *RSC Adv.* **2016**, *6*, 15441.
- (63) Ossenbach, A.; Rüegger, H.; Zhang, A.; Fischer, K.; Schluter, A. D.; Schmidt, M. Ion-induced stretching of low generation dendronized polymers with crown ether branching units. *Macromolecules* **2009**, *42*, 8781.
- (64) Mizusaki, M.; Endo, T.; Nakahata, R.; Morishima, Y.; Yusa, S.-i. pH-Induced Association and Dissociation of Intermolecular Complexes Formed by Hydrogen Bonding between Diblock Copolymers. *Polymers* **2017**, *9*, 367.
- (65) Berl, V.; Schmutz, M.; Krische, M. J.; Khoury, R. G.; Lehn, J. M. Supramolecular Polymers Generated from Heterocomplementary Monomers Linked through Multiple Hydrogen-Bonding Arrays-Formation, Characterization, and Properties. *Chem. Eur. J.* **2002**, *8*, 1227.
- (66) Orofino, T. A.; Flory, P. Relationship of the second virial coefficient to polymer chain dimensions and interaction parameters. *J. Chem. Phys.* **1957**, *26*, 1067.